Methods in Ecology and Evolution

MRS. LAURA STIDSHOLT (Orcid ID : 0000-0002-2187-7835)

Article type : Research Article

Handling editor: Professor Robert Freckleton

# A 2.6-gram sound and movement tag for studying the acoustic scene and kinematics of echolocating bats

LAURA STIDSHOLT*[1], MARK JOHNSON[1,2], KRISTIAN BEEDHOLM[1], LASSE JAKOBSEN[3], KATHRIN KUGLER[4], SIGNE BRINKLØV[1,3] ANGELES SALLES[5], CYNTHIA F. MOSS[5] & PETER TEGLBERG MADSEN[1,6].

1) Zoophysiology, Department of Bioscience, Aarhus University, Aarhus, Denmark
2) Scottish Oceans Institute, University of St Andrews, St Andrews, Scotland
3) Sound and Behaviour Group, Institute of Biology, University of Southern Denmark, Odense, Denmark
4) Department of Biologie II, Division of Neurobiology, Ludwig Maximilians University, 82152 Martinsried, Germany
5) Department of Psychological and Brain Sciences, Johns Hopkins University, Baltimore, MD 21218
6) Aarhus Institute of Advanced Studies, Høegh-Guldbergs Gade 6B, DK-8000 Aarhus C, Denmark

This article has been accepted for publication and undergone full peer review but has not been through the copyediting, typesetting, pagination and proofreading process, which may lead to differences between this version and the Version of Record. Please cite this article as doi: 10.1111/2041-210X.13108

## Abstract

**1.** To study sensorimotor behaviour in wild animals, it is necessary to synchronously record the sensory inputs available to the animal, and its movements. To do this, we have developed a biologging device that can record the primary sensory information and the associated movements during foraging and navigating in echolocating bats.

**2.** This 2.6 -gram tag records the sonar calls and echoes from an ultrasonic microphone, while simultaneously sampling fine-scale movement in three dimensions from wideband accelerometers and magnetometers. In this study, we tested the tag on an European noctula (*Nyctalus noctula*) during target approaches and on four big brown bats (*Eptesicus fuscus*) during prey interception in a flight room.

**3.** We show that the tag records both the outgoing calls and echoes returning from objects at biologically relevant distances. Inertial sensor data enables the detection of behavioural events such as flying, turning, and resting. In addition, individual wing-beats can be tracked and synchronized to the bat's sound emissions to study the coordination of different motor events.

**4.** By recording the primary acoustic flow of bats concomitant with associated behaviours on a very fine time-scale, this type of biologging method will foster a deeper understanding of how sensory inputs guide feeding behaviours in the wild.

## Keywords

Accelerometers, archival tag, auditory scene, bat echolocation, biologging, echogram, echoic scene, flight kinematics, inertial sensors, sensory-motor response.

## Introduction

Most behavioural patterns of animals are guided by sensory inputs that provide essential information about the surroundings. Quantifying the timing of sensory events is therefore crucial for understanding natural behaviours in the wild. However, animals are exposed to a barrage of sensory inputs in their natural habitats, and it is therefore difficult to quantify which cues are extracted to guide behaviour. This challenge is more tractable in echolocating bats, animals that perceive the world primarily by emitting high frequency calls and listening to the returning echoes. This actively generated sensory information and the concomitant motor patterns can be sampled at high resolution from free-flying bats by attaching lightweight sound and movement tags. Such technology can uncover how bats handle incoming streams of echoes, process that information, and respond with a set of vocal- and motor responses adapted to each new situation. Because of their small size (ca. 2-1000 gram) and costly mode of locomotion, bats can only tolerate extremely lightweight devices. As a consequence, detailed studies of bat sensory behaviour using on-board devices that capture both sonar calls and echoes are few. Most of our understanding of bat echolocation is based either on behavioural (*e.g.* Hartley, 1992; Surlykke & Kalko, 2008; Hiryu, Bates, Simmons, & Riquimaroux, 2010) and electrophysiological (*e.g.* Feng, Simmons, & Kick, 1978; Genzel, Hoffmann, Prosch, Firzlaff, & Wiegrebe, 2015) experiments in laboratories or on snapshots of bats passing by stationary microphone arrays and video cameras in the wild (*e.g.* Kalko & Schnitzler, 1993; Fujioka, Aihara, Sumiya, Aihara, & Hiryu, 2016). However, these methods cannot fully quantify the acoustic inputs available to free-flying bats nor the way echoes inform behaviour over longer time periods.

Despite the weight constraint, several radio-linked devices have been developed for bats (Patriquin, Leonard, Broders, & Garroway, 2010; Tsoar et al., 2011; Teague O'Mara, Wikelski, & Dechmann, 2014) to for example monitor heartrate (Studier & Howell, 1969; Dechmann, Ehret, Gaub, Kranstauber, & Wikelski, 2011) and movement (Richter & Cumming, 2008; Taylor et al., 2011; Dressler et al., 2016), but in only a few recent studies have acoustic recordings been possible. Radio-linked microphone tags have been used on *Pipistrellus abramus*, *Rhinolophus ferrumequinum nippon and Myotis myotis* to detect echoes from nearby structures or prey items in the laboratory (Mantani et al., 2012; Kinoshita et al., 2014; Budenz, Denzinger, & Schnitzler, 2018). However, the short operating range of telemetry microphones greatly restricts their use in the wild. More recently, self-recording acoustic tags have for the first time been deployed on free-flying birds (Anisimov et al., 2014) as well as numerous accelerometer tags have been deployed on different species in the wild (Nathan et al., 2012). Acoustic recording tags deployed on bats in the wild have advanced our understanding of how bats forage in the wild employing multimodal sensory integration (Danilovich et al., 2015) and group tactics (Cvikel et al., 2015). In addition to vocalizations, these tags measure GPS positions at 15 s intervals enabling studies of  overall movement patterns of bats foraging in the wild (Cvikel et al., 2014, 2015).

However, neither type of sound or movement tag has provided detailed information about the acoustic scene of bats in the form of echoes or their synchronous fine-scale movements, as required for studies of sensorimotor behaviours. This is due to either insufficient dynamic range to pick up echoes or at the same time to record fine-scale movements. For example, a bat may capture several insects in the 15 s time window (Griffin, Webster, & Michael, 1960) between successive GPS samples so while these positions track overall movements, they do not represent the rapid motor adjustments in flight behaviour as individual prey are selected, approached and captured. To gain a fine-scale sampling of the movement and the acoustic scene of bats, we have developed a high performance self-logging sound and movement tag to study sensorimotor behaviours in bats. This 2.6 g tag samples wideband sound from a microphone while simultaneously acquiring movement information from a high sample rate triaxial accelerometer and triaxial magnetometer. Here we use laboratory experiments on one European Noctule (*Nyctalus Noctula*) and four big brown bats (*Eptesicus fuscus*) to demonstrate that this tag achieves a dynamic range sufficient to capture both the outgoing calls and weak echoes returning from ecologically relevant objects and distances while enabling concomitant quantification of behaviours from inertial sensors with millisecond resolution. We also show that it is possible to estimate source levels (SLs) directly from on-board recordings, which is important when calculating detection ranges for passive acoustic monitoring and prey size with relevance for determining energy requirements, habitat preference and niche differentiation in the wild  (Fenton, Grinnell, Popper, & Fay, 2016).

## Tag design

The tag comprises a single custom-designed printed circuit board (PCB), onto which a battery and an ultrasonic microphone (Knowles FG-23329) are directly mounted with double-sided adhesive tape. The 0.5 mm thick fibreglass (FR4) PCB houses a microphone preamplifier, anti-alias filter, 16-bit analog-to-digital converter, accelerometer and an 8GB flash memory card. A low power digital signal processor on the board controls sampling of the sensors and performs loss-less compression and error-correction coding on the data streams before saving them to the flash memory. Data are offloaded and the battery recharged after trials via a miniature USB connector. The overall package measures 14 x 33 x 6 mm and weighs 2.6 gram with a 45 mAh lithium-ion rechargeable battery (Fig 1C). This size battery allows continuous recording at a sampling rate of 187.5 kHz for up to five hours. A larger battery enabling recordings of up to 8 hours increases the weight of the tag by approximately 0.5 gram. Currently, the microphone output is filtered by an 80 kHz 4-pole anti-aliasing filter, and a one pole 1 kHz high pass filter to reduce wind noise. An additional one pole high-pass filter in the microphone preamplifier gives a 10 dB increase in gain above 20 kHz to partially compensate for the reduced high frequency sensitivity of the microphone. The triaxial accelerometer (Analog Devices ADXL362 or Kionix KX022 configured for +/- 8g (+/- 78 $m/s^2$) full scale) is sampled at 1000 Hz (12 or 16 bit, respectively) with a 250 Hz anti-alias filter (AAF). The 3-axis magnetometer is sampled at 50 Hz without anti-alias filter as the sensor is turned off between samples. The lack of an AAF is acceptable because of the lower frequency content of magnetometer (i.e., orientation) data compared to acceleration (Martín López, Aguilar de Soto, Miller, & Johnson, 2016).

## Tag performance

The accelerometers were calibrated on a Brüel & Kjær shaker to establish frequency response and sensitivity. The microphone and preamplifier were calibrated by comparison with a 1/8” Brüel & Kjær microphone (See supplementary). After calibration, a whitening filter was computed to approximately correct the frequency response of the tag sound recording (Fig 1B, blue), and this post-emphasis filter was applied to all subsequent recordings. The average cliplevel of the tag and filter was 121 dB re 20 µPa (Fig

1B, red). The average noise-floor was -10 dB re 20 µPa$^2$/Hz (Fig 1B, blue, dashed) and 0 dB re 20 µPa$^2$/Hz before and after the whitening filter, respectively (Fig 1B). The noise floor integrated over the vocalization range of the study species (approx. 20 to 95 kHz) was 42 dB re 20 µPa RMS, resulting in an in-band dynamic range of 79 dB. The highest source level ever measured in a free-flying bat is 140 dB re 20 µPa at 0.1 m (Surlykke & Kalko, 2008), which is above the clipping level of the tag of 121 dB re 20 µPa. However, the position of the microphone behind the head means it receives these directional sounds far from the acoustic axis (Fig 4-5). On average, sound levels behind the head are 13 dB lower than the levels in front of the animal, and the tag should therefore be able to reliably record calls with SLs reaching up to 134 dB re 20 µPa at 0.1 m.

## Experiment 1: Target approach

The European noctule used in the study weighed from 26 to 30 grams that is the natural range of variation over a day. The tag weight thus represents between 7 and 10% of the body weight. Most studies report bat telemetry devices weighing between 5 to 10 % of the body mass (Teague O'Mara et al., 2014), and further studies are needed to establish both short term and long term effects of these loads. The tag was placed between the bats shoulders at the approximate centre of gravity (during flight) to minimize impact on movement and was attached to the fur using velcro. One side of the velcro was attached to the skin with a water-soluble glue (ÖkoNorm Pro Coll) (Fig 1A), while the other was attached to the tag. The velcro and glue added 0.3 gram extra weight. Despite the weight of the tag, the bat was able to perform a target approach with no visual impact on its flight manoeuvres. This bat was trained to land on a nylon sphere (d = 191mm, measured TS = -9dB at 0.1 m) anchored to a steel pole at 1.5 m height in a flight room (7 x 5 x 2.5 m) with low light level at the University of Southern Denmark. Simultaneous to the tag recording, audio data were also recorded with an array of nine ¼" G.R.A.S microphones (40BF) spaced by 0.5 meters and arranged in a cross 1 m behind the sphere (Fig 3A). All flights were recorded using video cameras (GoPro Hero2 at 720p and 30fps) and the array, tag, and video devices were synchronized by tapping on the microphones while filming both before and after the experiments. The bat was motivated by positive reinforcement with a mealworm reward immediately after each landing on the target sphere, which indicated a successful trial. The bat performed 34 successful target approaches in succession after initially missing the target during the first six trials after instrumentation. Total time spent with the tag attached was approximately 90 minutes (3 x ~30 minutes). The tag with velcro was removed with water to prevent skin irritation.

## The movement and acoustic scene of the bat during flight

The in-flight tag recordings show clear echoes from the target and other structures in the flight room (Fig 2A) but the presence of multiple echoes complicates the interpretation of the audio input on the tag. To facilitate interpretation of the auditory scene, we generated echograms (Johnson, Madsen, Zimmer, de Soto, & Tyack, 2004), to visualize the auditory scene of the bat as it approached the target (Fig 3). The flight path was reconstructed based on the time of arrival differences of each call at the microphone array behind the target sphere, and the changing spatial relationship between the bat and objects in the flight room can be tracked in the temporal pattern of echoes during the flight (Fig 3AB). Although cluttered, several echo streams are evident in the acoustic scene. An echo stream with a constant delay is seen from the beginning until one third into the flight. These are echoes from the wall parallel to the flight path of the bat. Some 700 ms before landing, a strong closing echo stream appears due to the target sphere, which the bat is approaching at approximately 3.5 m/s. However, at about the same time the auditory scene becomes more cluttered due to a mosaic of echoes returning from the microphone array, and the pillars and end wall of the flight room in addition to the target. The bat switches to a buzz (ICIs < 10 ms) some 100 ms before landing (Fig 3C). The sound and acceleration data recorded by the tag are tightly synchronized because both signals are sampled at rates that are derived from the same clock. This enables muscle movements such as wing beats to be aligned precisely with vocal output and echo features (Fig 3CD). Intervals of flight were reliably identified from the acceleration data when the z-axis acceleration varied cyclically with peak values above 50 m/s$^2$. Fourier transforms of the acceleration signals in the ventral-dorsal axis during flight intervals (n=39) were used to determine wing-beat frequency. Averaging all intervals, the wing-beat frequency was 10 to 16 beats/sec (Fig 3F).

A back-to-front transfer function (H) to calculate source levels on board

To reconstruct the emitted calls ahead of the flying animal from the calls received at extreme off-axis angles on the back-mounted tag, the same calls in the array and tag data were identified and compared in both the time (Fig 4) and frequency domain (Fig 5AB) for all flights. Sound levels were characterised in terms of Source Level (SL, i.e., the energy of calls recorded on the array, adjusted to a distance of 0.1 m in front of the bat) and Apparent Output Level (AOL, i.e., the energy in the calls recorded by the tag) (Madsen, Johnson, Aguilar de Soto, Zimmer, & Tyack, 2005). AOLs were on average 13 dB lower than the back-calculated on-axis SLs (difference between the intersections of the best fitting lines (Fig 4)). From the difference between the tag and the array recordings, we computed a back-to-front transfer function (H) (see supplementary) to approximate the call as it is emitted along the acoustic axis from the tag recording. The back-to-front corrected calls were broadly similar to those recorded on the array (Fig 4 red and Fig 5). The deviations may be ascribed to head movements and the placement of the tag that differed slightly between trials. Using the back-to-front transfer function, we calculated the target strength (TS) of the landing sphere based on eighteen landings using the tag-recorded call and echo pairs emitted 1 meter prior to landing (see supplementary). The mean of the TS estimates derived from the tag recordings (-8 dB at 0.1 m) was within 1 dB of the measured TS (-9 dB at 0.1 m) of the sphere.

**Experiment 2: Prey interception**

Four *Eptesicus fuscus* were trained to fly in a flight room (6 x 6 x 2 m) at the Johns Hopkins University, and catch tethered mealworms hanging from the ceiling in the centre of the room. As the bats weighed around 13 grams during the experimental days, the tags represented some 20 % of their body weights. *Eptesicus fuscus* have varying body weights naturally, as they are able to fly during late pregnancy and with their pups, which constitutes about a 20% increase in load (Kurta & Kunz, 1987). Thus, they appear able to carry substantial loads, at least in captivity. The bats were only instrumented approximately 25 minutes at a time and they all successfully captured their prey during the instrumentation. The bats were monitored carefully for any signs of discomfort or difficulty during the flight. Eight small mealworms were tethered together resulting in a combined TS of -42 dB @ 0.1 m. The interceptions were recorded by the tag and high-speed video cameras

(Phantom Miro M310 at 720p, at 100 fps and at 1280 x 800 resolution) to verify the fine-scale movement of the bats and the distances to the prey at each vocalization. In total, the bats performed 269 capture flights.

Acoustic scene of the bat during prey interception:

Synchronized audio, accelerometer and magnetometer data from one capture and subsequent landing on the flight room wall are displayed in Figure 7. In the visualized acoustic scene, the echo stream of the mealworms can be seen up to a distance of one meter just before prey capture at time 0 (Fig 7A). The closing echo stream from the wall prior to landing is more diffuse compared to the returning echo stream from the mealworms that are acoustical point-targets (Fig 7A). Even though the bat is flying in a large flight room, the target echoes further than approximately one meters distance are buried in clutter echoes from the walls, floor and ceiling. Echo-to-clutter levels as recorded by the tag are likely worse than experienced by the bat due to the omnidirectional receiving characteristics of the microphone in comparison to the directional hearing of bats at the frequencies in question. The dynamic range of the echogram is 85 dB enabling calculations of echo levels down to 10 dB re 20 $\mu Pa^2 s$ with these signals. Echoes could be extracted out to a median distance of 0.65 m, and to a maximum distance of 1.2 m based on all flights by the four *Eptesicus fuscus* (Fig 8). The variation in distances for the same target is owing to the different source levels of the bats, as well as their individual capturing strategies introducing clutter at different ranges in the flight room.

Fine-scale movements during prey interception:

The manoeuvring during prey capture can be viewed by combining the z-axis acceleration (Fig 7C) and tri-axial magnetometer signals (Fig 7D). Here, the capture is indicated by a powerful stroke immediately followed by a rotation of the body axis (Fig 7D, red) and a turn towards the starting point on the wall (Fig 7D yellow). The high-speed video recordings were used to verify these movements. The pitch and roll one second before and after each prey capture event were also extracted (Fig 9). The increase in pitch at the time of prey capture marks the forward flexion of the interfemoral membrane to seize the prey (Fig 9A). Shortly thereafter, the bat rolls to either side while it simultaneously changes its direction (Fig 9B). This movement has been approximated in a dead-reckoning track (Fig 10), showing how the bat changes its direction and returns to the wall just after prey capture. Dead reckoned tracks can be used to analyse the foraging technique and tortuosity performed during prey capture events (Madsen et al., 2013).

Dead-reckoned tracks require an estimate of the speed of the animal, which can be difficult to acquire reliably (Wilson et al., 2007). However, for prey-captures and landings, the speed of the bat can be approximated from the closing speed of the echoes (Fig 3) improving the accuracy of fine-scale tracking.

## Discussion

To study how behaviour is guided by sensory inputs in wild animals, it is necessary to record the sensory information available to, and extracted by, the animal, along with its motor patterns. Here, we have developed a tag that enables synchronous recordings of the acoustic output (Fig 3BC), the movement (Fig 3DE) and the actively generated echo scene of free flying bats for four hours or more depending on battery (Fig 2-3BC). It has previously only been possible to study wild bat behaviour and their echo returns from small targets by relating video recordings of movement with acoustic data recorded by far-field microphones (Geberl, Brinkløv, Wiegrebe, & Surlykke, 2015; Warnecke, Chiu, Engelberg, & Moss, 2015; Sumiya et al., 2017). Such fixed systems are very limited in their ability to sample the behavior of individual wild bats that use echo information to guide prey captures and flight over large distances in complex environments. We demonstrate that an on-board tag can detect echoes from individual targets such as prey as well as the walls, floor and ceiling of the flight room, enabling these features to be tracked in echograms that visually represent the actively generated auditory scene of the bat during flight (Fig 3B and Fig 7A). Moreover, the flying motions of the bat can be related directly to the range to each echo source to allow for the examination of how bats navigate towards targets or around obstacles.

The capability of the tag to record over the full bandwidth of many bat calls means that the complete signal of returning echoes is acquired. In this case, discrete echoes were recorded from a wall at a distance of 10 m (Fig 2) off the target sphere (TS = - 8dB at 0.1 m) at 2.5 m and off 8 small tethered mealworms (TS = - 42 dB) at one meters distance. (Moss, Bohn, Gilkenson, & Surlykke, 2006). As bats increase their SLs in the wild by up to 25 dB (Surlykke et al., 1993) compared to the lab, echoes reflected off prey that have similar TS will likely be recorded with a similar signal to noise ratio out to 3 meters in open space in the wild.

The frequency-dependent differences introduced by recording off the acoustic axis (Fig 4-5) highlight the importance of considering the frequency-dependent difference in level between front and back when analysing full bandwidth calls and estimating absolute SLs. By using a back-to-front transfer function to correct the outgoing calls recorded by the tag, SLs can be estimated from tag recordings, enabling estimation of the detection range of calls in passive acoustic surveys as well as prey target strength. Using this approach, we derived a TS for the sphere from the tag recordings that was within 1 dB of the measured TS, showing that such target size estimations are reliable. However, more importantly, this result also demonstrates that the call levels recorded by the tag are closely related to SL enabling studies of SL adaptation to target strength, clutter or interfering noise in the wild because both SL and TS as a function of range, noise and clutter can be measured by the tag.

Although accelerometers have been used on the larger Old World fruit bats (*Pteropididae*) (Fahr et al., 2015), this is to our knowledge the first accelerometer and magnetometer data recorded from echolocating bats. Flying and resting are readily detected in these data enabling studies of time allocation and energy use (Fig 6), and more advanced classification tools will likely enable the construction of increasingly fine scale ethograms in the future. Individual wing beats during flight generate strong oscillatory z-axis accelerations with magnitude of 25 to 70 $m/s^2$ for both species, which is well-above previous estimates of acceleration and deceleration during flights found in other bat species (Aldridge, 1987). The average wing-beat frequency of all flights varied between 10 and 16 beats/s (Fig 3F), which is somewhat faster than previously measured in the same species (Bruderer & Popa-Lisseanu, 2005). Wing-beat frequency also changed during a single flight depending on the task (Fig 3E). Thus, using a combination of triaxial accelerometers and magnetometers, it would be possible to analyse how bats power flight, manoeuver and change direction and orientation during prey interception (Fig 9-10) in the wild, where it is not possible to use high-speed video cameras to capture these behaviours. At 2.6 grams, the tag is too heavy for use on bats below the size of *Nyctalus noctula* and *Eptesicus fuscus* the species used in the present study. To achieve a recording time covering a full night of foraging, a tag weight of 3.5 grams is required, which limits the choice of appropriate species in the wild. Although the trained bats from two species in this study successfully landed and captured prey, without overt sign of being encumbered by the tag, longer attachments, even on larger species, would require attention to potential behavioural and energetic impacts of the tag. However, many species of bats change their body weight up to 30 % naturally between feeding and fasting cycles suggesting that they may be resilient to carrying relatively heavy loads for shorter time periods in the wild (Aldridge & Brigham, 1988). Indeed sound tags with a similar weight relative to body weight (11-14 %) applied to wild bats have successfully recorded foraging behaviour (Cvikel et al., 2015). Moreover, the new data generated by this type of method may provide an impetus for further miniaturization and potentially integration with GPS as already used by Cvikle and co-workers (2015). Most of the tag weight is in the circuit board (1.5 g with components) of which a single component, the memory chip, accounts for 0.6 g. The board uses off-the-shelf components and standard fabrication methods, which are economical, but more expensive chip-on-board or system-on-chip approaches could substantially reduce the weight and dimensions of the tag increasing the range of species for which it is suitable.

In conclusion, we have shown that this type of multisensory, miniature tag provides a new tool for analysing the actively generated acoustic scene of free-flying echolocating bats engaged in natural behaviours in complex natural environments. Specifically, this method will allow for quantification of feeding rates and prey capture success rates of wild bats and even echolocating birds, and address how they handle multiple echo streams, select between prey items, avoid clutter and reverberation, reject interference patterns, and perform decision-making to inform behavioural transitions in the wild. As the weight of this type of technology is reduced, it will be possible to draw significant inferences about the metabolic expenditure, physiology and communication of bats and birds in the wild over longer time periods that can inform management and conservation.

## Acknowledgements

This study was supported by the Carlsberg Foundation via a Semper Ardens grant, ONR, N00014-17-1-2736; AFOSR FA9550-14-1-0398, and NSF NCS-FO: 1734744 and a Human Frontiers Science Program Long-Term Fellowship to AS. These experiments were approved by The Danish Council for Experiments on Animals under permit number: 2016-15-0201-00989 and by the Johns Hopkins University Animal Care and Use Committee under protocol number BA17A107. We thank Uwe Firzlaff and Lutz Wiegrebe for their help.

## Data Accessibility

Data deposited in the Dryad repository: http://datadryad.org/resource/doi:10.5061/dryad.s1r7qr3

## Author contributions

L.S. conducted the experiments, analyzed the data and wrote the manuscript. M.J designed and manufactured the tag; contributed to interpretation and analysis of data and to writing of the manuscript. K.B. analyzed and interpreted the data. L.J., S.B., K.K trained the bats, conducted the experiments and revised the paper. A.S trained the bats and conducted experiments; C.F.M. and A.S. helped with data interpretation and drafting of the manuscript. P.T.M. designed the experiment, contributed to the analysis and interpretation of data and writing of the manuscript. All authors contributed to writing the manuscript.

**Materials & Correspondence**. Correspondence to Laura Stidsholt by laura.stidsholt@bios.au.dk.

## References

Aldridge, H. D. J. N. (1987). Body accelerations during wingbeat in six bat species: The function of the upstroke in thrust generation. *Journal of Experimental Biology*, *130*(2), 275–293.

Aldridge, H. D. J. N., & Brigham, R. M. (1988). Load Carrying and Maneuverability in an Insectivorous Bat: A Test of The 5% ‘Rule’ of Radio-Telemetry. *Journal of Mammalogy*, *69*(2), 379–382.

Anisimov, V. N., Herbst, J. A., Abramchuk, A. N., Latanov, A. V, Hahnloser, R. H. R., & Vyssotski, A. L. (2014). Reconstruction of vocal interactions in a group of small songbirds. *Nature Methods*, *11*(11), 1135–1137. doi:10.1038/nmeth.3114

Bruderer, B., & Popa-Lisseanu, A. G. (2005). Radar data on wing-beat frequencies and flight speeds of two bat species. *Acta Chiropterologica*, *7*(1), 73–82. doi:10.3161/1733-5329(2005)7[73:RDOWFA]2.0.CO;2

Budenz, T., Denzinger, A., & Schnitzler, H.-U. (2018). Reduction of emission level in approach signals of greater mouse-eared bats (*Myotis myotis*): No evidence for a closed loop control system for intensity compensation. *PLoS ONE*, *13*(3), e0194600. doi:10.1371/journal.pone.0194600

Cvikel, N., Egert Berg, K., Levin, E., Hurme, E., Borissov, I., Boonman, A. M., & Yovel, Y. (2015). Bats aggregate to improve prey search but might be impaired when their density becomes too high. *Current Biology*, *25*(2), 206–211. doi:10.1016/j.cub.2014.11.010

Cvikel, N., Levin, E., Hurme, E., Borissov, I., Boonman, A. M., Amichai, E., & Yovel, Y. (2014). On-board recordings reveal no jamming avoidance in wild bats. *Proceedings of the Royal Society of London, 282*(1798), 20142274–20142274. doi:10.1098/rspb.2014.2274

Danilovich, S., Krishnan, A., Lee, W.-J., Borrisov, I., Eitan, O., Kosa, G., & Yovel, Y. (2015). Bats regulate biosonar based on the availability of visual information. *Current Biology*, *25*(23), R1124–R1125. doi:10.1016/j.cub.2015.11.003

Dechmann, D. K. N., Ehret, S., Gaub, A., Kranstauber, B., & Wikelski, M. (2011). Low metabolism in a tropical bat from lowland Panama measured using heart rate telemetry: an unexpected life in the slow lane. *The Journal of Experimental Biology*, *214*, 2605–3612. doi:10.1242/jeb.056010

Dressler, F., Ripperger, S., Hierold, M., Nowak, T., Eibel, C., Cassens, B., & Kölpin, A. (2016). From radio telemetry to ultra-low power sensor networks: Tracking bats in the wild. *IEEE Communications Magazine*, *54*(1), 129–135. doi:10.1109/MCOM.2016.7378438

Fahr, J., Abedi-Lartey, M., Esch, T., Machwitz, M., Suu-Ire, R., Wikelski, M., & Dechmann, D. K. N. (2015). Pronounced seasonal changes in the movement ecology of a highly gregarious central-place forager, the African Straw-Coloured Fruit Bat (*Eidolon helvum*). *PLoS ONE*, *10*(10), e0138985. doi:10.1371/journal.pone.0138985

Feng, A. S., Simmons, J. A., & Kick, S. A. (1978). Echo detection and target-ranging neurons in the auditory system of the bat, *Eptesicus fuscus*. *Science*, *202*(4368), 645–648. doi:10.1126/science.705350

Fenton, B. M., Grinnell, A. D., Popper, A. N., & Fay, R. R. (2016). *Bioacoustics*. (B. M. Fenton, A. D. Grinnell, A. N. Popper, & R. R. Fay, Eds.). New York: Springer Publishing.

Fujioka, E., Aihara, I., Sumiya, M., Aihara, K., & Hiryu, S. (2016). Echolocating bats use future-target information for optimal foraging. *PNAS*, 1–5. doi:10.1121/1.4898428

Geberl, C., Brinkløv, S., Wiegrebe, L., & Surlykke, A. (2015). Fast sensory–motor reactions in echolocating bats to sudden changes during the final buzz and prey intercept. *Proceedings of the National Academy of Sciences*, *112*(13), 4122–4127. doi:10.1073/pnas.1424457112

Genzel, D., Hoffmann, S., Prosch, S., Firzlaff, U., & Wiegrebe, L. (2015). Biosonar navigation above water II: exploiting mirror images. *Journal of Neurophysiology*, *113*(4), 1146–1155. doi:10.1152/jn.00264.2014

Griffin, D. R., Webster, F. A., & Michael, C. R. (1960). The echolocation of flying insects by bats. *Animal Behaviour*, *8*, 141–154. doi:10.1016/0003-3472(60)90022-1

Hartley, D. J. (1992). Stabilization of perceived echo amplitudes in echolocating bats. I. Echo detection and automatic gain control in the big brown bat, *Eptesicus fuscus*, and the fishing bat, *Noctilio leporinus*. *The Journal of the Acoustical Society of America*, *91*(2), 1120–32. doi:10.1121/1.402639

Hiryu, S., Bates, M. E., Simmons, J. A., & Riquimaroux, H. (2010). FM echolocating bats shift frequencies to avoid broadcast-echo ambiguity in clutter. *Proceedings of the National Academy of Sciences of the United States of America*, *107*(15), 7048–7053. doi:10.1073/pnas.1000429107

Johnson, M. P., Madsen, P. T., Zimmer, W. M. X., de Soto, N. A., & Tyack, P. L. (2004). Beaked whales echolocate on prey. *Proceedings of the Royal Society B: Biological Sciences*, *271*, S383–S386. doi:10.1098/rsbl.2004.0208

Kalko, E. K. V., & Schnitzler, H.-U. (1993). Plasticity in echolocation signals of European pipistrelle bats in search flight: implications for habitat use and prey detection. *Behavioral Ecology and Sociobiology*, *33*(6), 415–428. doi:10.1007/BF00170257

Kinoshita, Y., Ogata, D., Watanabe, Y., Riquimaroux, H., Ohta, T., & Hiryu, S. (2014). Prey pursuit strategy of Japanese horseshoe bats during an in flight target selection task. *Journal of Comparative Physiology A*, *200*, 799–809. doi:10.1007/s00359-014-0921-3

Kurta, A., & Kunz, H. T. (1987). Size of bats at birth and maternal investment during pregnancy. *Symposia of the Zoological Society of London*, *57*, 79–106.

Madsen, P. T., Johnson, M. P., Aguilar de Soto, N., Zimmer, W. M. X., & Tyack, P. L. (2005). Biosonar performance of foraging beaked whales (Mesoplodon densirostris). *Journal of Experimental Biology*, *208*(2), 181–194. doi:10.1242/jeb.01327

Madsen P.T., Aguilar de Soto, N., Arranz, P. and Johnson, M. (2013), “Echolocation in Blainville’s beaked whales (Mesoplodon densirostris)”. *Journal of Comparative Physiology A*, 199(6): 451-469. doi: 10.1007/s00359-013-0824-8

Mantani, S., Hiryu, S., Fujioka, E., Matsuta, N., Riquimaroux, H., & Watanabe, Y. (2012). Echolocation behavior of the Japanese horseshoe bat in pursuit of fluttering prey. *Journal of Comparative Physiology*, *198*(10), 741–751. doi:10.1007/s00359-012-0744-z

Martín López, L. M., Aguilar de Soto, N., Miller, P., & Johnson, M. (2016). Tracking the kinematics of caudal-oscillatory swimming: a comparison of two on-animal sensing methods. *The Journal of Experimental Biology*, *219*(14), 2103–2109. doi:10.1242/jeb.136242

Moss, C. F., Bohn, K., Gilkenson, H., & Surlykke, A. (2006). Active listening for spatial orientation in a complex auditory scene. *PLoS ONE*, *4*(4), e79. doi:10.1371/journal.pbio.0040079

Nathan, R., Spiegel, O., Fortmann-Roe, S., Harel, R., Wikelski, M., & Getz, W. M. (2012). Using tri-axial acceleration data to identify behavioral modes of free-ranging animals: general concepts and tools illustrated for griffon vultures. *The Journal of Experimental Biology*, *215*, 986–996. doi:10.1242/jeb.058602

Patriquin, K. J., Leonard, M. L., Broders, H. G., & Garroway, C. J. (2010). Do social networks of female northern long-eared bats vary with reproductive period and age? *Behavioral Ecology and Sociobiology*, *64*(1), 899–913. doi:10.1007/S00265-0

Richter, H. V., & Cumming, G. S. (2008). First application of satellite telemetry to track African straw-coloured fruit bat migration. *Journal of Zoology*, *275*(2), 172–176. doi:10.1111/j.1469-7998.2008.00425.x

Stidsholt, L., Johnson, M., Beedholm, K., Jakobsen, L., Kugler, K., Brinkløv, S., Salles, A., Moss, C. F., Madsen, P. T. (2018). Data from: A 2.6-gram sound and movement tag for studying the acoustic scene and kinematics of echolocating bats. Methods in Ecology and Evolution doi:10.5061/dryad.s1r7qr3

Studier, E. H., & Howell, D. J. (1969). Heart rate of female big brown bats in flight author. *American Society of Mammalogists*, *50*(4), 842–845. doi:10.2307/1378280

Sumiya, M., Fujioka, E., Motoi, K., Kondo, M., Hiryu, S., Egelhaaf, M., & Bischof, H. (2017). Coordinated control of acoustical Field of view and flight in three-dimensional space for consecutive capture by echolocating bats during natural foraging. *PLoS ONE*, *12*(1), e0169995. doi:10.1371/journal.pone.0169995

Surlykke, A., & Kalko, E. K. V. (2008). Echolocating bats cry out loud to detect their prey. *PLoS ONE*, *3*(4), e2036. doi:10.1371/journal.pone.0002036

Surlykke, A., Miller, L. A., Møhl, B., Andersen, B. B., Christensen-Dalsgaard, J., & Buhl Jørgensen, M. (1993). Echolocation in two very small bats from Thailand: *Craseonycteris thonglongyai* and *Myotis siligorensis*. *Behavioral Ecology and Sociobiology*, *33*(1), 1–12. doi:10.1007/BF00164341

Taylor, P. D., Mackenzie, S. A., Thurber, B. G., Calvert, A. M., Mills, A. M., McGuire, L. P., & Guglielmo, C. G. (2011). Landscape movements of migratory birds and bats reveal an expanded scale of stopover. *PLoS ONE*, *6*(11), e27054. doi:10.1371/journal.pone.0027054

Teague O'Mara, M., Wikelski, M., & Dechmann, D. K. N. (2014). 50 years of bat tracking: Device attachment and future directions. *Methods in Ecology and Evolution*, *5*(4), 311–319. doi:10.1111/2041-210X.12172

Tsoar, A., Nathan, R., Bartan, Y., Vyssotski, A., Dell'Omo, G., & Ulanovsky, N. (2011). Large-scale navigational map in a mammal. *Proceedings of the National Academy of Sciences*, *108*(37), E718–E724. doi:10.1073/pnas.1107365108

Warnecke, M., Chiu, C., Engelberg, J., & Moss, C. F. (2015). Active listening in a bat cocktail party: Adaptive echolocation and flight behaviors of Big brown bats, *Eptesicus fuscus,* foraging in a cluttered acoustic environment. *Brain, Behavior and Evolution*, *86*, 6–16. doi:10.1159/000437346

Wilson, R. P., Liebsch, N., Davies, I. M., Quintana, F., Weimerskirch, H., Storch, S., Lucke, K., Siebert, U., Zankl, S., Müller, G., Zimmer, I., Scolaro, A., Campagna, C., Plötz, J., Bornemann, H., Teilmann, J., & McMahon, C. R. (2007). All at sea with animal tracks; methodological and analytical solutions for the resolution of movement. *Deep-Sea Research II, 54,* 193-210. doi:10.1016/j.dsr2.2006.11.017

## Figure legends

**Fig 1: Cliplevel and noise-floor of the microphone subsystem.** Power spectral densities of the maximum input level (i.e., the clipping level (CL), solid lines) and the noise-floor (dashed lines) of the tag (blue lines) and of the tag with post-emphasis filtering to correct the spectrum (red lines). The difference between the pair of red lines indicates the 1 Hz band dynamic range. The noise-floor was estimated from a running FFT of a 10 sec long signal with an FFT length of 256 with a window length of 256 and an overlap size of 128 samples.

**Fig 2: Illustration of echoic scene of one bat call.** A) Spectrogram of an outgoing call and returning echoes. Strong echoes are evident from the target sphere at 2.5 meters distance. However, echoes from the microphone array and the flight room's ceiling, floor and walls at up to 7.5 meters distance increase the complexity of the auditory scene. High frequency attenuation of sound due to absorption (hum: 90% and temp: 20 degrees) (B) is evident in the echoes returning from longer distances (A). Elevated noise levels at 80 kHz throughout the spectrogram are due to the higher noise floor at this frequency after equalization of the tag recording to compensate for the microphone response. The spectrogram was produced with an FFT length of 512 with a window length of 256 and an overlap of 128 samples at 250 kHz and a dynamic range of the colour map of 70 dB set by the difference between the maximum energy and the median energy of the spectra.

**Fig 3: Combined, synchronized sound (ABC) and movement (DEF) data from one flight of the *European noctula*.** A) The bat's flight path towards the nylon target sphere (black) based on the time of arrival of the calls emitted and recorded by a microphone array behind the target. Calls are color-coded according to their energy. Buzz calls emitted approximately one meter before landing could not be extracted from the array recordings. B) Echogram showing the dynamic echoic scene of the bat as recorded by the tag during the approach flight to the nylon target sphere. Sound envelopes corresponding to each outgoing call are represented by vertical coloured bars and displayed in the horizontal axis at the production time of the call (Johnson et al., 2014). The visual resolution matches the temporal resolution of the bat as the width of the bars are spaced according to the intercall intervals. The vertical axis represents the time delay between emission of a call and return of the echoes. Delay is expressed as distance to the object by multiplying with half the speed of sound in air. Echoes reflected off the nylon sphere and off background structures are marked. C) Source levels (SLs) of calls during the flight. The colours indicate the instantaneous call rate in calls/sec. Notice the decrease in SL as the repetition rate increases. The buzz is initiated when the intercall interval ~ 10 ms (blue colours). Echo levels (ELs) from the target sphere are shown from some two meters before landing (black). D) The wing movement of the bat during the flight is shown by the acceleration in the z-dimension. Notice the synchronization of calls and wing beats. E) Spectrogram of z-axis accelerometer data over the same time interval. The wingbeat frequencies vary according to the position of the bat: Approximately two meters before landing (at -0.8 sec) the wingbeat frequency increases from 10 to 15 beats/sec. This corresponds to when the bat is ascending towards the sphere. The spectrogram was produced with a colour map dynamic range of 20 dB and an FFT length of 2048 with a window length of 256 and an overlap of 200 samples at 488 samples/sec. F) The average wing-beat frequency from 155 flights is between 10 to 15 wing-beats/sec.

**Fig 4: Amplitude correction for the tag placement.** The offset between recording off-axis (on tag microphone) and on-axis (on microphone array) is illustrated by the linear relationship between AOL and SL (blue circles). The regression line is shown in blue ($r^2$= 0.84). After correction using the back to front transfer function, the corrected AOLs, SLs and the linear regression are shown in red ($r^2$= 0.84). All energy measurements were calculated in dB re 20 µ$Pa^2$s over a 98 % energy window. Note the 13 dB offset between the two regression lines.

**Fig 5: Frequency correction for the tag placement.** An average of 252 spectra is shown for the tag recorded calls (purple), for the tag recorded calls after correction for the frequency response of the microphone (blue), after correction for the placement of the tag on the back behind the sound source (red), and for the same calls recorded on the array (yellow). Illustrations of the time domain representation of the same calls and where they are recorded from are shown in the insertion.

**Fig 6: Example of behaviours in the laboratory.** Acceleration in three dimensions showing characteristic patterns during flight and resting.

**Fig 7: Acoustic scene and fine-scale movement during target interception and subsequent landing of *Eptesicus fuscus*.** A) An echogram illustrating the auditory streams impinging onto the bat during flight. Echoes reflected off the mealworms can be seen in the last second before prey capture out to a distance of one meter, whereas the more diffuse echo stream from the wall can be seen prior to landing at time 2 seconds.

B) Outgoing calls (coloured) and returning energy (black) during the flight. The calls are color-coded according to the inter-call intervals. Echoes from the mealworms out to a distance of one meter have been extracted (black). C) Z-axis acceleration showing how the bat takes off, flies stereotypically across the room, and manoeuvres to capture the prey at time 0. The powerful wingbeat 100 ms before prey capture guides the rotation to the prey measured by the magnetometers. D) Tri-axial magnetometers showing the orientation of the bat using Euler angles. The bat is flying towards the prey and returning to where it came from. This is indicated by the heading changing from positive to negative just after prey capture (yellow). In addition, the bat is rolling just after prey capture as it is manoeuvring back to where it came from (red).

**Fig 8: Histogram of the maximum detection distance of prey echoes from *Eptesicus fuscus.*** The distance at which the last echo can be extracted in the echogram of each flight have been pooled together for all 269 captures of the five bats. In approximately 8 % of the captures, the echoes were not traceable in our recordings. The median detection distance is 0.65 m (red line).

**Fig 9: Movement during prey capture by *Eptesicus fuscus.*** Pitch (A) and roll (B) one second before and after prey interception for all flights (grey) and the mean of all flights (black) (N = 269).

**Fig 10: Dead reckoning track of one prey capture by *Eptesicus fuscus.*** By combining triaxial accelerometer and magnetometer data, the flight path of the bat can be approximated. The bat takes off from the wall, flies towards the tethered mealworm, catches the prey and turns around towards the wall. This track overall matches the track as judged by video.

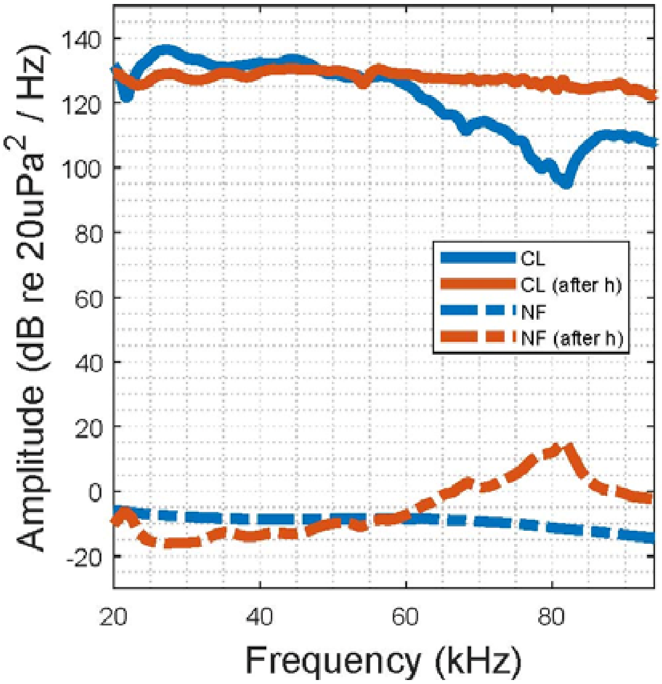
Amplitude (dB re 20uPa$^2$ / Hz)
140
120
100
80
60
40
20
0
-20
20
40
60
80
Frequency (kHz)
CL
CL (after h)
NF
NF (after h)

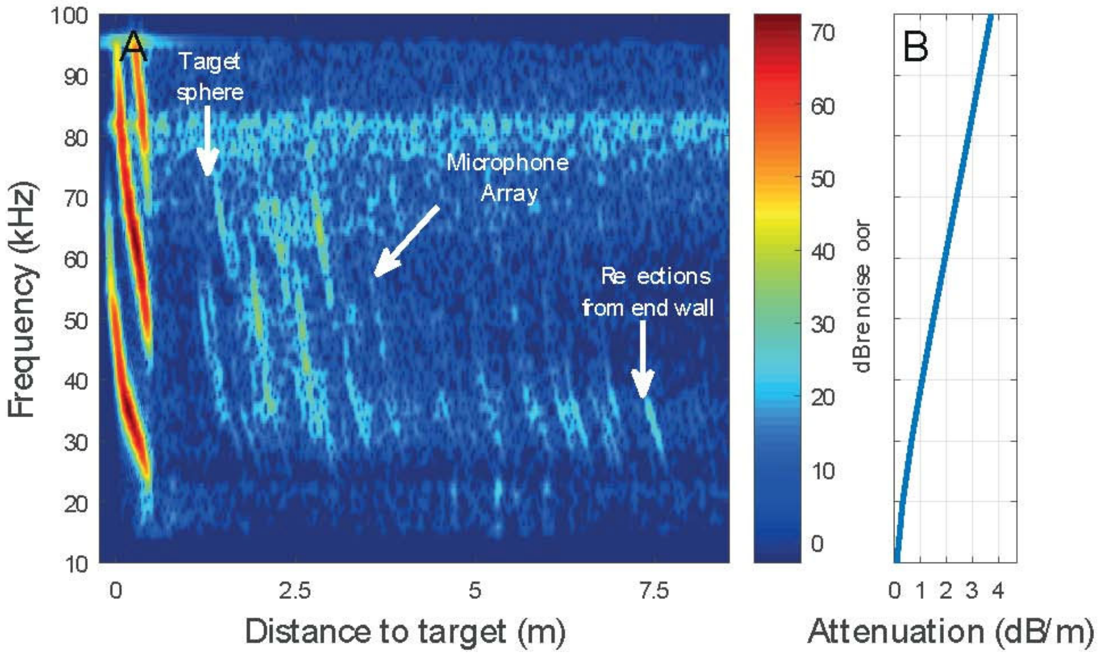
A
B
Target sphere
Microphone Array
Reflections from end wall
Frequency (kHz)
100
90
80
70
60
50
40
30
20
10
0
2.5
5
7.5
Distance to target (m)
70
60
50
40
30
20
10
0
dB re noise floor
0 1 2 3 4
Attenuation (dB/m)

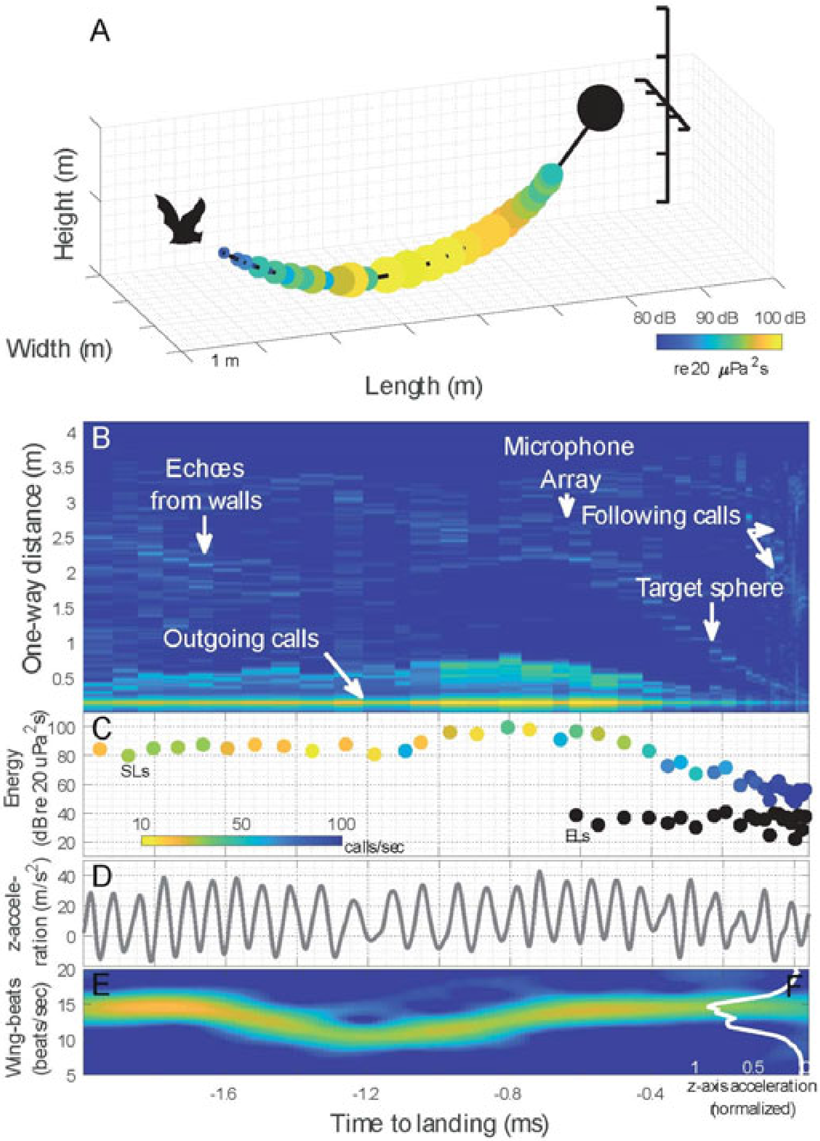
A
Height (m)
Width (m)
Length (m)
1 m
80 dB
90 dB
100 dB
re 20 $\mu$Pa$^2$s
B
One-way distance (m)
4
3.5
3
2.5
2
1.5
1
0.5
Echœs from walls
Microphone Array
Following calls
Target sphere
Outgoing calls
C
Energy (dB re 20 uPa$^2$s)
100
80
60
40
20
SLs
ELs
10
50
100
calls/sec
D
z-acceleration (m/s$^2$)
40
20
0
E
F
Wing-beats (beats/sec)
20
15
10
5
-1.6
-1.2
-0.8
-0.4
1
0.5
0
z-axis acceleration (normalized)
Time to landing (ms)

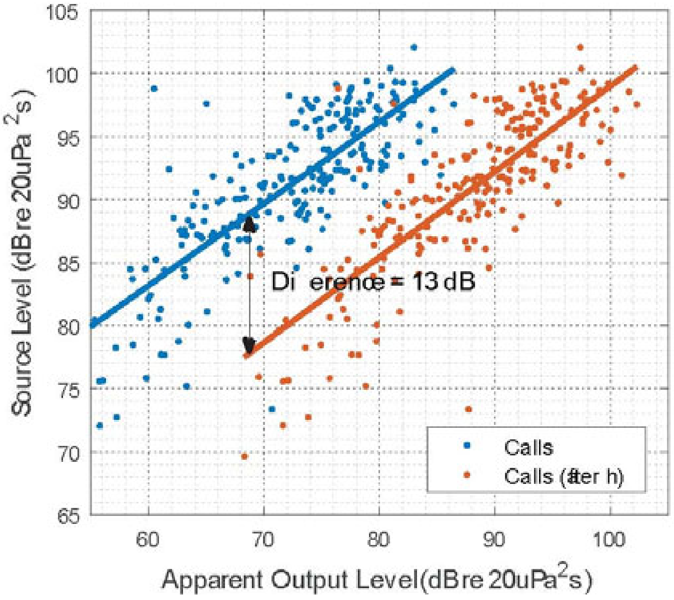
105
100
95
90
85
80
75
70
65
Source Level (dBre 20uPa $^2$s)
60
70
80
90
100
Apparent Output Level (dBre 20uPa$^2$s)
Difference = 13 dB
Calls
Calls (after h)

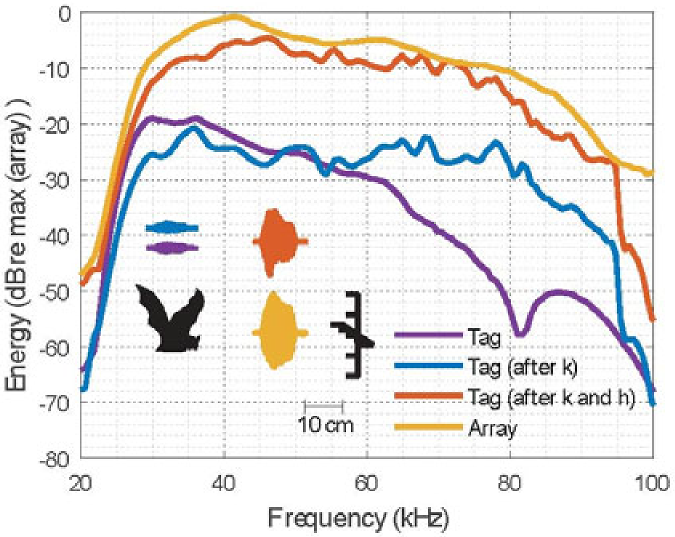
0
-10
-20
-30
-40
-50
-60
-70
-80
Energy (dBre max (array))
20
40
60
80
100
Frequency (kHz)
10 cm
Tag
Tag (after k)
Tag (after k and h)
Array

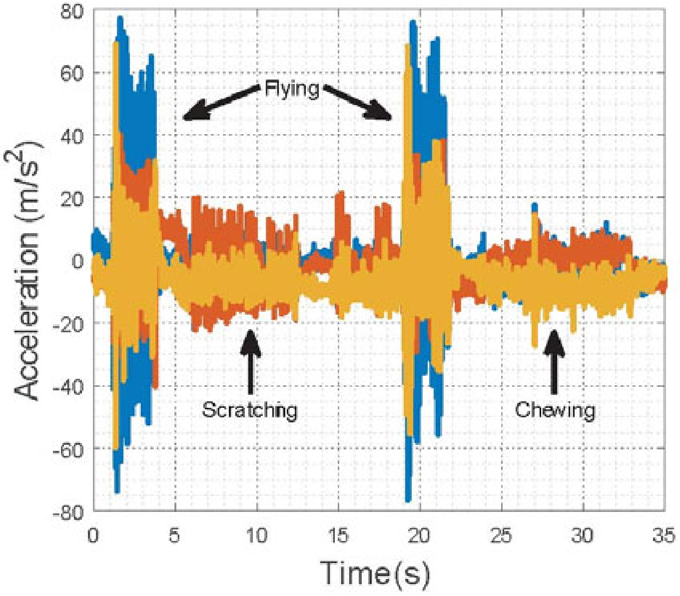
80
60
40
20
0
-20
-40
-60
-80
Acceleration (m/s²)
0
5
10
15
20
25
30
35
Time(s)
Flying
Scratching
Chewing

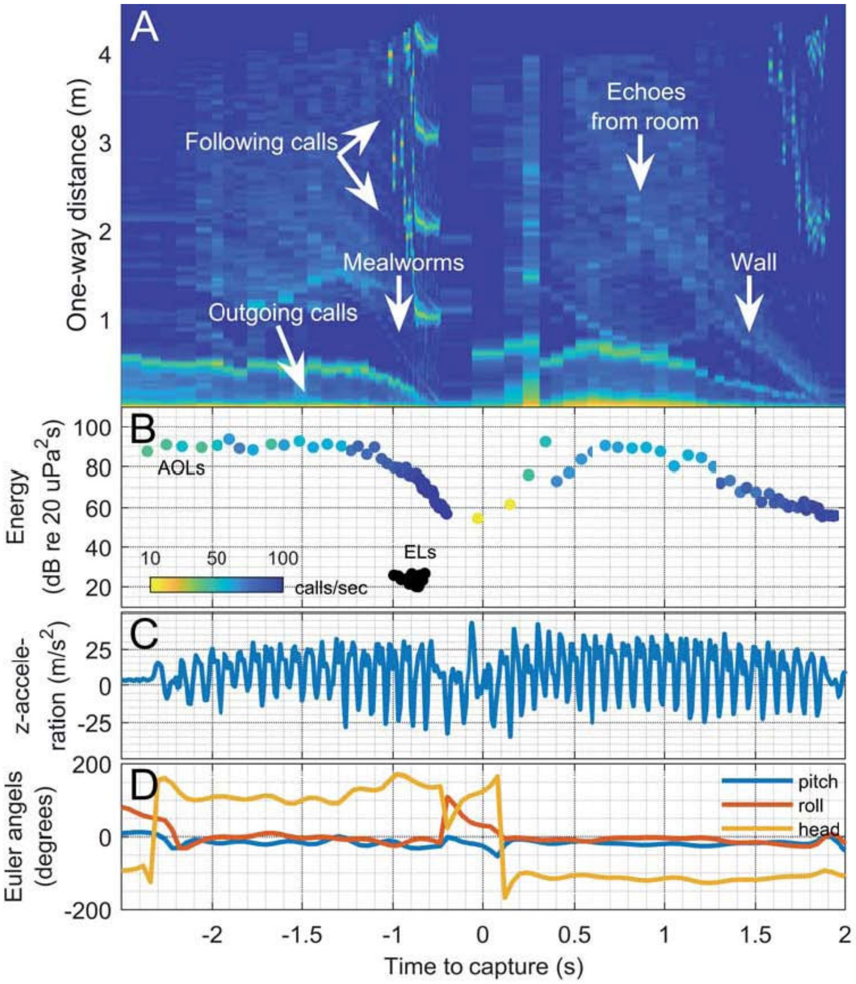
A
One-way distance (m)
4
3
2
1
Following calls
Echoes from room
Mealworms
Wall
Outgoing calls
B
Energy (dB re 20 uPa$^2$s)
100
80
60
40
20
AOLs
ELs
10
50
100
calls/sec
C
z-acceleration (m/s$^2$)
25
0
-25
D
Euler angels (degrees)
200
0
-200
pitch
roll
head
-2
-1.5
-1
0
0.5
1
1.5
2
Time to capture (s)

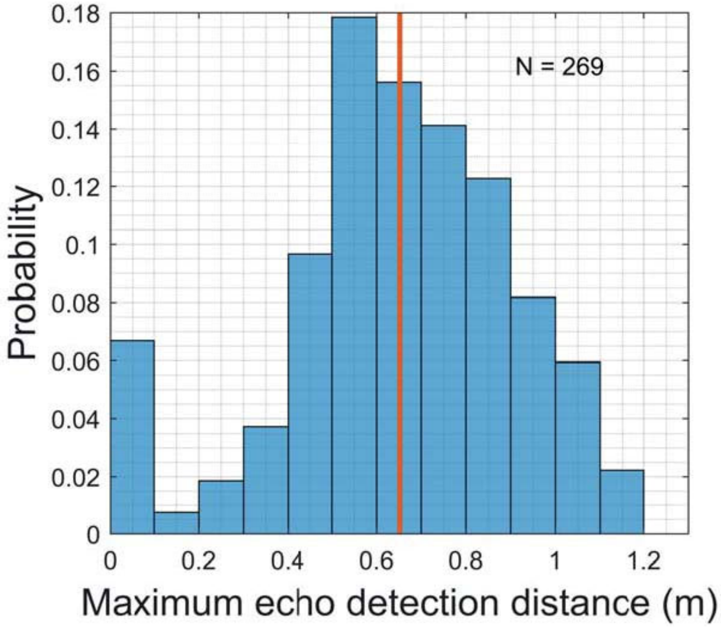
N = 269
Probability
0.18
0.16
0.14
0.12
0.1
0.08
0.06
0.04
0.02
0
0
0.2
0.4
0.6
0.8
1
1.2
Maximum echo detection distance (m)

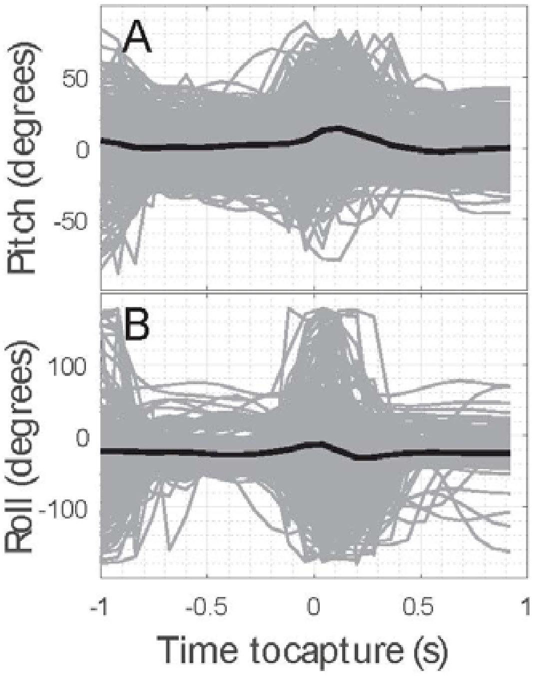
A
Pitch (degrees)
50
0
-50
B
Roll (degrees)
100
0
-100
-1
-0.5
0
0.5
1
Time tocapture (s)

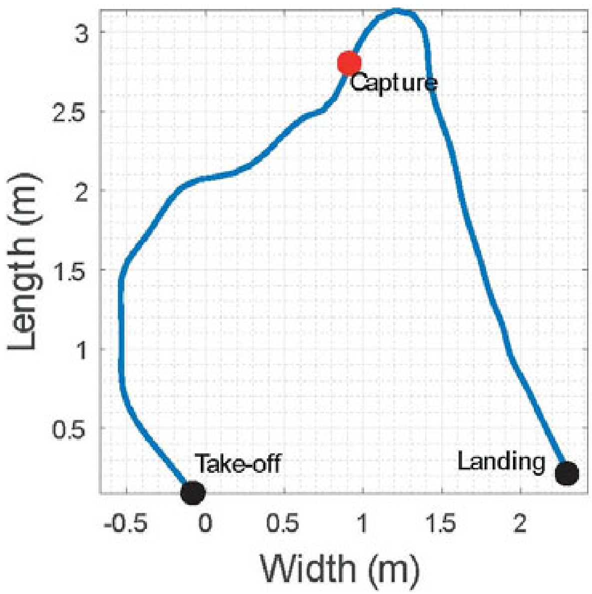
Capture
Take-off
Landing
Length (m)
Width (m)
3
2.5
2
1.5
1
0.5
-0.5
0
0.5
1
1.5
2